

g factors of high spin states in $^{154,155}\text{Er}$ and ^{157}Yb and the nature of the neutron $\frac{13}{2}^+$ quasiparticle in transitional nuclei

M. H. Rafailovich,* O. C. Kistner, and A. W. Sunyar
Brookhaven National Laboratory, Upton, New York 11973

S. Vajda and G. D. Sprouse

Physics Department, State University of New York at Stony Brook, Stony Brook, New York 11790

(Received 30 November 1983)

The g factors of the $I^\pi=11^-$ isomer in ^{154}Er and $I^\pi=\frac{13}{2}^+$ isomers in ^{155}Er and ^{157}Yb were measured using the technique of time-dependent perturbed angular distributions. The value obtained for ^{154}Er , $g=+0.0154(12)$, indicates a predominant configuration of $\nu[i_{13/2}, h_{9/2}]_{10^-, 11^-}$ for the isomeric state. The results for ^{155}Er and ^{157}Yb , $g=-0.085(5)$ and $g=-0.116(12)$, respectively, are explained in terms of Pauli blocking of the 3^- core excitation component in the wave function of the $\frac{13}{2}^+$ state.

I. INTRODUCTION

There has been extensive recent work in the region around $A=150$ aimed at elucidating the structure of nuclei at large angular momentum. For $N < 87$ the yrast states that have been studied so far appear to consist mainly of proton and neutron quasiparticles coupled to large angular momenta, while for $N > 87$ some of the angular momentum also results from the collective rotation of the deformed nucleus. The $\frac{13}{2}^+$ states observed in odd neutron nuclei in this region can either be made up from neutron $i_{13/2}$ orbitals, or by coupling either $h_{9/2}$ or $f_{7/2}$ neutron orbitals to the 3^- excitation. Since the 3^- excitation in this region is thought to be primarily a proton excitation, g-factor determinations of these odd neutron states should be sensitive to the admixture of this 3^- state in the quasiparticle structure. As the number of $h_{11/2}$ protons in the valence shell increases, a strong diminution of the amount of 3^- admixture in the $\frac{13}{2}^+$ states should be observed because of Pauli blocking.

In general, with the exception of a small region near Gd where the $4f$ shell is half-filled, information on nuclear moments of high spin states in the rare earth region is sparse and difficult to obtain because of the paramagnetic relaxation of the nuclear alignment by the unpaired $4f$ electrons. The present measurements outside of this region have been made possible because of the very small g

factors of the particular neutron states studied. The relaxation rate, which is proportional to g^2 , was sufficiently long in these cases to allow observation of the Larmor oscillations. It is hoped that these Er nuclei can now be utilized as probes with which to determine which host materials are most effective at preserving the nuclear alignment so that g-factor measurements can be extended to other Er nuclei with larger g factors, as well as to other rare earth nuclei.

II. EXPERIMENTAL METHOD

Heavy ion beams from the Brookhaven National Laboratory Tandem Van de Graaff were used to populate the isomers and implant them into a Pb foil backing. The target-backing combination was attached to the cold finger of a Joule-Thomson cooling device and placed in an external magnetic flux density of 2.49(5) T pointing in the vertical direction. Adjustment of the beam steering to correct for deflection by the magnetic field was accomplished with the help of a scintillating focusing screen. The temperature of the backing was measured with a thermocouple. The uncertainty in the temperature due to beam heating was estimated to be no larger than 2 deg. Table I gives the target-beam combinations for each isomer studied, and Fig. 1 shows the relevant decay schemes. The beam was in all cases pulsed with a repetition period

TABLE I. Summary of relevant data for each isomer.

Nucleus	Reaction	E_{beam} [MeV]	I^π	$t_{1/2}$ [ns]	E_γ [keV] ^a
^{154}Er	$^{121}\text{Sb}(^{37}\text{Cl}, 4n)$	154	11^-	40(3)	625, 601, 560, 542, 688
^{155}Er	$^{121}\text{Sb}(^{37}\text{Cl}, 3n)$	154	$\frac{13}{2}^+$	30(2)	532
^{157}Yb	$^{144}\text{Sm}(^{16}\text{O}, 3n)$	88	$\frac{13}{2}^+$	45(3)	494

^aTransitions used for obtaining $R(t)$. See the text.

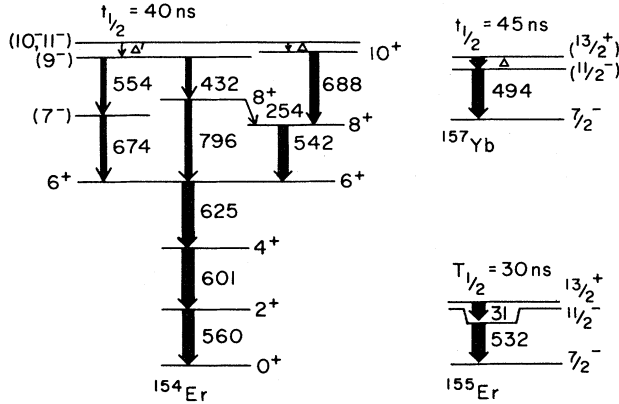


FIG. 1. Partial decay schemes from isomers in ^{154}Er (Ref. 7) and ^{155}Er and ^{157}Yb (Ref. 11).

of $0.5 \mu\text{s}$. Two 18% efficient Ge(Li) detectors were placed at $\pm 135^\circ$ to the beam direction in the horizontal plane. The fast timing signals from the Ge(Li) detectors were used to start a common time to amplitude converter which was stopped by a signal from the beam pulsing system. The time resolution of the system on a single gamma-ray line was 5 ns. Each event consisted of a time signal and one of the two Ge(Li) energy signals. The spectra were stored directly into two 512×128 (energy \times time) matrices at a rate of 10 kHz. The photopeaks of interest were corrected for underlying Compton backgrounds by subtracting the appropriately normalized adjacent flat regions of the gamma spectra. The time spectra of the two counters $I(\theta, t)$ were then combined to form the ratio

$$R(t) = \frac{I(+135^\circ, t) - I(-135^\circ, t)}{I(+135^\circ, t) + I(-135^\circ, t)}. \quad (1)$$

III. EXPERIMENTAL RESULTS

Figure 2 shows the time dependence of the ratio function, $R(t)$, for ^{154}Er at three different temperatures. A reversed field run at 297 K (not shown) shows the expected phase reversal. ^{155}Er was populated simultaneously with ^{154}Er by the $(^{37}\text{Cl}, 3n)$ reaction branch, and $R(t)$ at 297 K for this nucleus is shown in Fig. 3. Figure 4 shows $R(t)$ for ^{157}Yb at 297 K and two opposite directions of the applied magnetic field. The data were fit with the function

$$R(t) = \frac{3A_2G_2(t_0)e^{-\lambda_2 t} \sin(2\omega_L t + \phi)}{4 + A_2G_2(t_0)e^{-\lambda_2 t}}, \quad (2)$$

where A_2 is the amplitude of the P_2 Legendre polynomial in the angular distribution due to the alignment from the nuclear reaction. The attenuation coefficient, $G_2(t_0)$, accounts for any loss of alignment during the slowing down process, and $e^{-\lambda_2 t}$ accounts for paramagnetic relaxation of the alignment by the fluctuating paramagnetic fields. The phase shift, ϕ , takes into account the angular deviation of the beam from 0° due to the magnetic field. Two aspects of the data are evident. First, the Larmor fre-

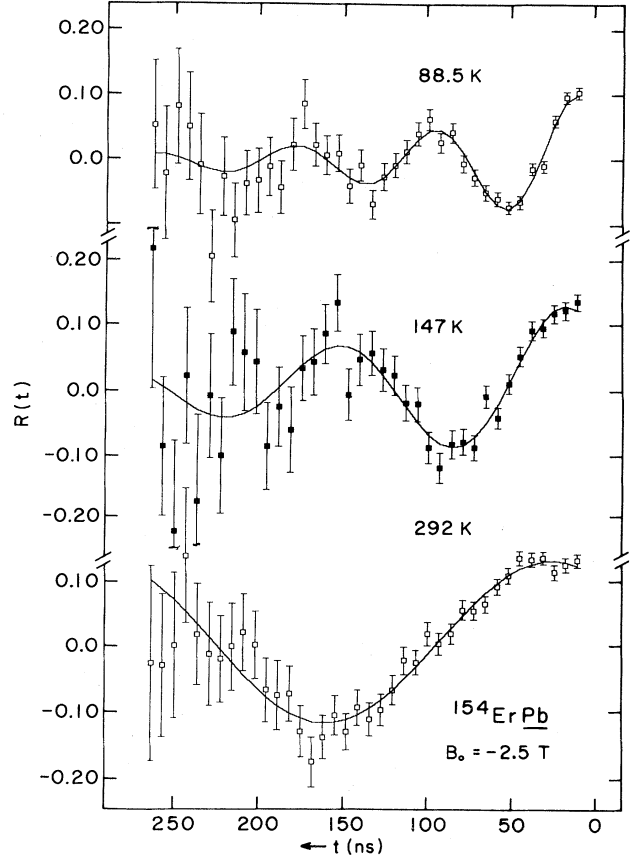


FIG. 2. $R(t)$ for ^{154}Er at three different temperatures in an external field of $B = -2.49 \text{ T}$.

quency is strongly temperature dependent, and second, the time dependence of the oscillation amplitude exhibits increased relaxation at the lower temperatures. Both of these effects are expected for paramagnetic Er ions.

A. Magnetic g factors

The Larmor frequency, ω_L , is given by $\omega_L = g\mu_N B_{\text{eff}}/\hbar$. The externally applied field, B_0 , is modified by the

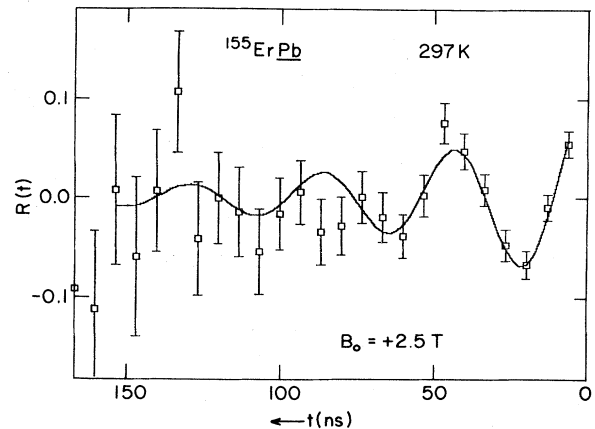


FIG. 3. $R(t)$ for ^{155}Er at $T = 297 \text{ K}$ and $B = +2.49 \text{ T}$.

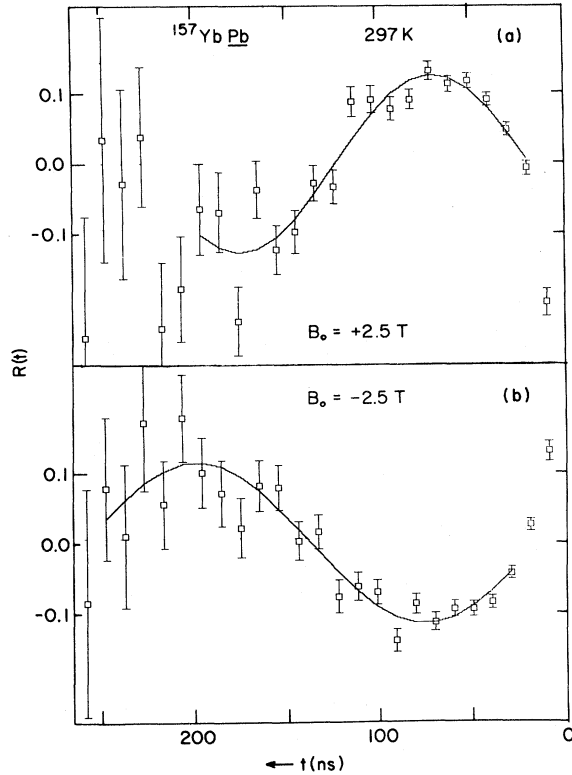


FIG. 4. $R(t)$ for ^{157}Yb at $T=297$ K with (a) $B = +2.49$ T and (b) $B = -2.49$ T.

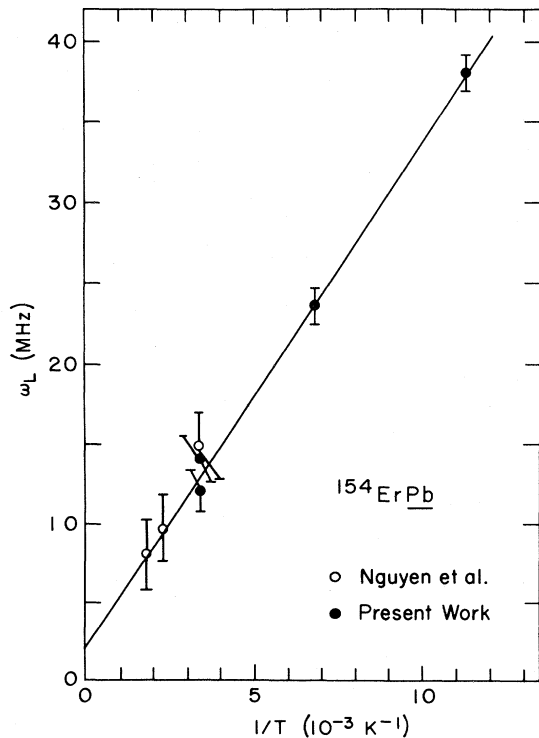


FIG. 5. ω_L vs $1/T$ for $^{154}\text{ErPb}$. The shaded points are from the present work. The open circles are from Ref. 1.

TABLE II. Summary of results for the $I^\pi = 11^-$ isomer in ^{154}Er .

Temp. [K]	ω_L^a [MHz]	λ_2 [μs^{-1}]	$A_2G_2(t_0)$
292	14.2(14) ^a	3(3)	0.21(7)
292	12.2(14) ^b	2(4)	0.21(9)
147	24.1(11)	5(2)	0.19(2)
88.5	38.0(11)	9(2)	0.16(2)

^a $B = +2.49(5)$ T.

^b $B = -2.49(5)$ T.

paramagnetic ion as a function of temperature, resulting in an effective field at the nucleus that can be represented by an expression of the form

$$B_{\text{eff}} = B_0 \left[\alpha + \frac{\chi}{T} \right]. \quad (3)$$

Figure 5 is a plot of the Larmor frequency as a function of $1/T$ for ^{154}Er . The shaded points, which extend the data to 523 K, are taken from Ref. 1. The straight line is a fit to $\omega_L = \omega_0[\alpha + (\chi/T)]$, where $\omega_0 = g\mu_N B_0/\hbar$. The fit parameters obtained were $\chi\omega_0 = 3.15(17) \times 10^3$ MHz K and $\alpha\omega_0 = 2.4(12)$ MHz. The data are well fit by a straight line throughout the experimental temperature range, an indication that the system is a good paramagnet, with the Er impurity in a unique charge state. We assume for the Er impurity ion² a charge state of +3, and use the calculations of Ref. 2, which give $\chi = 1750$ with an error of 5%. We find³ $g(^{154}\text{Er}) = +0.0152(12)$ and $\alpha = 0.13(6)$. The same values were also used to extract the g factor of ^{155}Er .

In the case of ^{157}Yb , the Larmor frequency was found to be independent of temperature, an indication that the Yb impurity ion was in the Yb^{+2} ionic state, in which case there is no paramagnetic enhancement of the applied field. That Yb ions exist in the +2 ionization state in metals is well known from previous Mössbauer effect measurements.⁴ Table II summarizes the data for ^{154}Er and Table III lists the g factors measured for the $I = \frac{13}{2}^+$ states in ^{155}Er , ^{157}Yb , and for completeness,⁵ ^{147}Gd .

B. Paramagnetic relaxation

The measured values of the relaxation constants, λ_2 , for ^{154}Er are listed in Table II. The relaxation constant is related to the g factor and to the internal field, B_{int} , at $T=0$ through the relation⁶

TABLE III. g factors of $I^\pi = \frac{13}{2}^+$ states.

Nucleus	Z	g	a^2
^{147}Gd	64	$-0.037(11)^a$	0.41(17)
^{155}Er	68	$-0.085(5)$	0.24(10)
^{157}Yb	70	$-0.116(12)$	0.13(6)

^aReference 5.

$$G_2(t) = G_2(t_0)e^{-\lambda_2 t}, \quad (4a)$$

by

$$\lambda_2 = (2\tau_c / \hbar^2) g^2 \mu_N^2 B_{\text{int}}^2, \quad (4b)$$

where τ_c is the spin flip correlation time of the paramagnetic ion.

A plot of λ_2 vs $1/T$ for $^{154}\text{Er}(11^-)$ is shown in Fig. 6, along with the $A_2 G_2(t_0)$ data for the same nucleus. The appropriate precession frequency in Eq. (4a) is not the average frequency, ω_L , but rather the instantaneous frequency, ω_0 , in the fluctuating internal field B_{int} . Since this frequency and the nuclear quantities are independent of temperature, the linear variation of λ_2 with $1/T$ implies that τ_c is proportional to $1/T$. In metals, τ_c can be related to the density of states at the Fermi level, $\rho(E_f)$, by the expression

$$\tau_c = [4\pi / \hbar |\rho(E_f) J|^2 kT]^{-1}. \quad (5)$$

Using the measured g factor for ^{154}Er , we can deduce this parameter for Er in Pb as $|\rho(E_f) J| = 0.023(3)$. This value is very similar to that determined⁵ for Gd in Pb. The observed relaxation time, τ_{relax} , for nuclear alignment of Er in Pb at temperature T can be related to the nuclear g factor by the expression

$$\tau_{\text{relax}} = \frac{T [\text{K}]}{3450 g^2} \text{ ns}. \quad (6)$$

It is clear that for proton states with g factors of order 1, the nuclear alignment will be relaxed at room temperature in times of the order of 100 ps, while for neutron states with g factors less than 0.1, the alignment can survive for 10 ns or more. A host material with somewhat

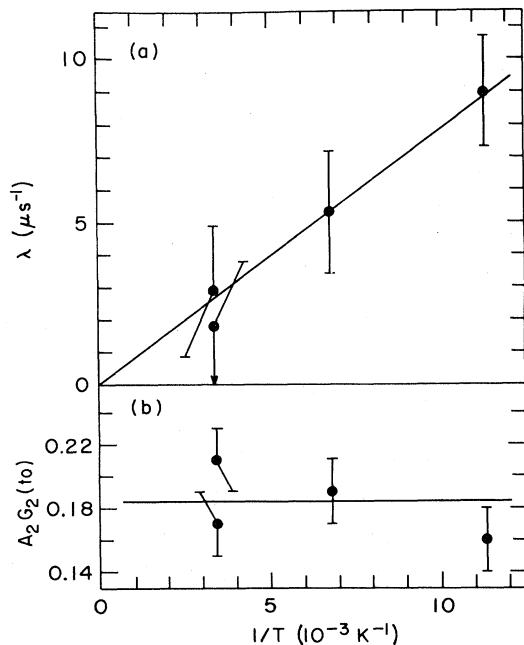


FIG. 6. (a) λ_2 vs $1/T$ for $^{154}\text{ErPb}$; (b) the anisotropy extrapolated to $t=0$, $A_2 G_2(t_0)$ vs $1/T$.

higher $\rho(E_f)$ and consequently faster fluctuation time, τ_c , would allow longer relaxation times, and could appreciably extend the number of different isomeric states in the erbium isotopes that could be measured.

IV. DISCUSSION

A. ^{154}Er

Figure 1 shows the decay⁷ of the 11^- isomer in ^{154}Er . Gamma-ray spectroscopy measurements alone require an I^π assignment of 10^- or 11^- for this isomer. On the basis of systematics with the neighboring $N=86$ nuclei, 11^- is preferred.⁸ In this region various combinations of the $f_{7/2}$, $h_{9/2}$, and $i_{13/2}$ neutron orbitals and the 3^- octupole phonon are possible. The effective g factors of these states are listed in Table IV. The $i_{13/2}$ value was obtained from the average of all the measurements listed in Ref. 9. The actual experimental uncertainty in each case is no larger than 10%, but as is shown in Ref. 10 for a given nuclear core, polarization effects can spread the $i_{13/2}$ g factor from 0.14 to 0.17. Since the magnitudes of these core effects are unknown in this region, a conservative error covering the whole range is given. The effective $h_{9/2}$ single particle value is not known experimentally and was calculated using standard parameters $g_I(\nu) = -0.03(3)$ and $g_S(\nu) = 0.6(1)g_S(\text{free})$ from the Gd region.⁵

Table V summarizes the possible configurations for the isomer together with the calculated g factors. From this table it can be seen that the small magnitude of the g factor requires a predominant configuration for the isomeric level of $\nu[i_{13/2}, h_{9/2}]_{10^-, 11^-}$, where the antiparallel orientation of the intrinsic spins of the two neutrons results in a vanishingly small magnetic moment. Although the difference between the experimental and calculated values is within the uncertainties of the parameters used, there may also be a contribution from small admixtures of single particle states coupled to the 3^- core excitation. The effect of core admixtures on the lower-lying $\frac{13}{2}^+$ states in the odd- N nuclei is discussed in the next subsection.

TABLE IV. Effective single particle g factors.

Orbital	g factor	Nucleus
$\nu f_{7/2}$	$-0.39(2)^a$	^{143}Nd
$\nu i_{13/2}$	$-0.15(2)^b$	$^{192, 195, 196, 198, 200, 205, 206}\text{Pb}$, $^{193, 195, 197, 199}\text{Hg}$
$\nu h_{9/2}$	$+0.18(4)^c$	
3^- core excitation	$+0.62(12)^d$	^{146}Gd

^aReference 9.

^bThis value represents an average derived from the values listed for the corresponding nuclei in Ref. 9. The error reflects uncertainties in core-polarization effects discussed in Ref. 10.

^cCalculated assuming $g_I(\nu) = -0.03(3)$, $g_S = 0.6(1)g_S(\text{free})$ from Ref. 5.

^dReference 5.

TABLE V. Possible configurations for the negative parity isomer in ^{154}Er .

Configuration	g_{calc}
$\nu[i_{13/2}, h_{9/2}]11^-$	-0.015(45)
$\nu[i_{13/2}, h_{9/2}]10^-$	-0.021(45)
$\nu[i_{13/2}, f_{7/2}]10^-$	-0.20(3)
$[3^- \times \nu(f_{7/2}, h_{9/2})8^+]11^-$	+0.17(6)
$[3^- \times \nu(h_{9/2})^2 8^+]11^-$	+0.30(3)
Experimental value	+0.0152(15)
	+0.017(3) ^a

^aReference 1.

B. ^{155}Er and ^{157}Yb

Figure 1 shows the decay schemes¹¹ of the $\frac{13}{2}^+$ isomers in ^{155}Er and ^{157}Yb . In both cases only the two transitions shown are observed and the assigned multipolarities are based on angular distribution data, lifetime considerations, and known conversion coefficients.² An $I^\pi = \frac{9}{2}^-$ assignment for the isomer is considered unlikely since, (a) the sign and magnitude of the measured g factors for ^{155}Er , $g = -0.085(5)$, and for ^{157}Yb , $g = -0.116(12)$, are totally inconsistent with the calculated value of $g(\nu h_{9/2}) = +0.18(4)$; (b) the relative moments of inertia of the $N=87$ nuclei¹² do not indicate that the cores are sufficiently deformed as to affect the degeneracy of the $i_{13/2}$ orbital and bring the $\frac{1}{2}^-(660)$ orbital to the Fermi surface.

Due to the low energy of the 3^- core excitations in the $A \sim 150$ region, the $\frac{13}{2}^+$ isomeric levels are expected to be admixed with a $(3^- \times \nu f_{7/2})$ particle-core excitation component.⁴ The amount of admixture is difficult to determine from spectroscopic studies. The $E1/E3$ branching ratio has not been measured for any of the cases discussed in this work. A search in the present work for the $E3$ crossover transition in ^{155}Er yielded only an upper limit of 1% of the $E1$ intensity. Furthermore, even if this branching ratio were known, the interpretation is not straightforward and depends on some model dependent phase factors. In contrast, g -factor measurements are much more sensitive to small configuration admixtures.

The g factor of the $\frac{13}{2}^+$ level can be parametrized as

$$g(\frac{13}{2}^+) = a^2 g[3^- \times \nu f_{7/2}] + (1 - a^2) g(\nu i_{13/2}), \quad (7)$$

*Present address: Weizmann Institute of Science, Department of Nuclear Physics, Rehovot, Israel.

¹L. Nguyen, H. Sergolle, P. Auger, G. Auger, G. Bastin, T. Lönnroth, J. P. Thiband, and L. Thome, *Z. Phys. A* **309**, 207 (1983).

²C. Gunther and I. Lindgren, in *Perturbed Angular Correlations*, edited by E. Karlsson, E. Matthias, and K. Siegbahn, (North-Holland, Amsterdam, 1964), p. 355; also R. E. Watson (private communication).

³Preliminary results on this g factor were reported by us in the

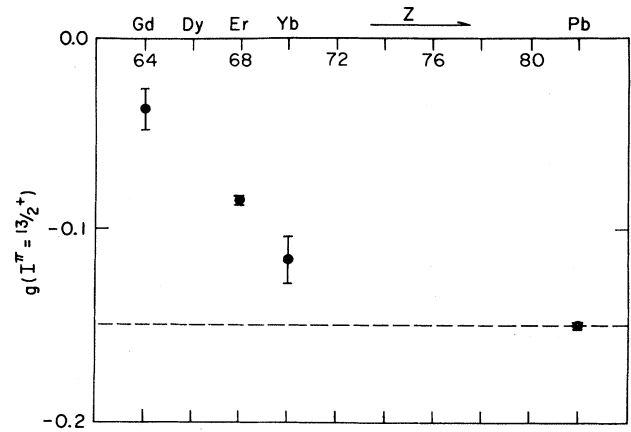


FIG. 7. Measured g factors of $I^\pi = \frac{13}{2}^+$ states in the $A \sim 150$ region as a function of Z . The value for ^{147}Gd is from Ref. 5.

where a is the amplitude of the corresponding term in the wave function. Table III summarizes the values of a^2 for the $N=83$ nucleus, ^{147}Gd and for the $N=87$ nuclei, ^{155}Er and ^{157}Yb . These values were calculated by assuming the single particle g factors listed in Table IV. Figure 7 is a plot of measured g factors of the $\frac{13}{2}^+$ states as a function of Z . From the figure one can see that as more proton pairs are added to the $Z=64$ core the experimental g factor monotonically approaches the effective single particle value for the $\nu i_{13/2}$ orbital. This may plausibly be interpreted as being due to the Pauli blocking of the $\pi[d_{5/2}^{-1}, h_{11/2}]$ quasiparticle component in the 3^- core excitation. Theoretical calculations⁴ have shown that the amplitude of this component in the core excitation is greater than 50%. Consequently, as more proton pairs are added to the $h_{11/2}$ subshell, fewer orbitals become available for the core excitation, the energy of the 3^- excitation increases, and a decreased admixture into the $\frac{13}{2}^+$ state results. An opposite effect is expected with the addition of more neutron pairs to the $N=82$ core, which should lower the energy of the 3^- level due to the proton-neutron interaction. To determine these effects more quantitatively, work is in progress on the g factor of ^{149}Dy which is only two protons away from ^{147}Gd .

This research was carried out under the auspices of the U. S. Department of Energy under Contract No. DE-AC02-76CH00016.

Proceedings of the ORNL Conference on High Angular Momentum Properties of Nuclei, 1982, Vol. 1, p. 48. A refinement of the errors on g and a quoted here was made possible by the inclusion of the results from Ref. 1 in the data analysis. From only the high temperature data, a value of $g = +0.017(3)$ is obtained in Ref. 1.

⁴A. Palenzona, *J. Less-Common Met.* **21**, 443 (1970); Willem Mattens, Ph.D. thesis, Amsterdam University, 1980.

⁵O. Häusser, H.-E. Mahnke, T. K. Alexander, H. R. Andrews, J. F. Sharpey-Schafer, M. L. Swanson, D. Ward, P. Taras,

- and J. Keinonen, Nucl. Phys. **A379**, 287 (1982).
- ⁶M. E. Caspari, S. Frankel, and G. T. Wood, Phys. Rev. **127**, 1519 (1962).
- ⁷C. Baktash, E. der Mateosian, O. C. Kistner, and A. W. Sunyar, Phys. Rev. Lett. **42**, 637 (1979).
- ⁸A. W. Sunyar, Phys. Scr. **24**, 298 (1981).
- ⁹*Table of Isotopes*, 7th ed., edited by C. M. Lederer and V. S. Shirley (Wiley, New York, 1978).
- ¹⁰C. H. Stenzel, H. Grawe, H. Haas, H.-E. Mahnke, and K. H. Maier (unpublished).
- ¹¹C. Baktash, D. Horn, E. der Mateosian, O. C. Kistner, and A. W. Sunyar (unpublished).
- ¹²C. Baktash, in *High Angular Momentum Properties of Nuclei*, edited by N. R. Johnson (Harwood, New York, 1982), p. 207.
- ¹³P. Kleinheinz, Phys. Scr. **24**, 236 (1981).